

Article

A Novel Design and Development of a Strip-Fed Circularly Polarized Rectangular Dielectric Resonator Antenna for 5G NR Sub-6 GHz Band Applications

Usman Illahi ^{1,*}, Javed Iqbal ^{1,2}, Muhammad Irfan ³, Mohamad Ismail Sulaiman ⁴,
Muhammad Abbas Khan ⁵, Abdul Rauf ⁶, Inam Bari ⁷, Mujeeb Abdullah ⁸, Fazal Muhammad ^{9,*},
Grzegorz Nowakowski ¹⁰ and Adam Glowacz ¹¹

- ¹ Electrical Engineering Department, FET, Gomal University, Dera Ismail Khan 29050, KP, Pakistan; javediqbal.iet@gu.edu.pk
 - ² School of Electrical and Electronic Engineering, Engineering Campus, Universiti Sains Malaysia, Nibong Tebal 14300, Penang, Malaysia
 - ³ Electrical Engineering Department, College of Engineering, Najran University, Najran 61441, Saudi Arabia; miditta@nu.edu.sa
 - ⁴ Advanced Telecommunication Technology, Communication Technology Section, British Malaysian Institute, Universiti Kuala Lumpur, Gombak 53100, Selangor, Malaysia; mismail@unikl.edu.my
 - ⁵ Department of Electrical Engineering, Balochistan University of Information Technology, Engineering and Management Sciences, Quetta 87300, Pakistan; muhammad.abbas@buitms.edu.pk
 - ⁶ Department of Electrical Engineering, National University of Sciences and Technology, H-12, Islamabad 44000, Pakistan; a.rauf@nust.edu.pk
 - ⁷ Systems Engineering Department, Military Technological College, Muscat 111, Oman; inam.bari@mtc.edu.om
 - ⁸ School of Aeronautical and Electrical Engineering, College of Aeronautical Engineering, National University of Science and Information Technology, Risalpur 24080, Pakistan; mabdullah@cae.nust.edu.pk
 - ⁹ Electrical Engineering Department, University of Engineering and Technology, Mardan 23200, Pakistan
 - ¹⁰ Faculty of Electrical and Computer Engineering, Cracow University of Technology, Warszawska 24 Str., 31-155 Kraków, Poland; gnowakowski@pk.edu.pl
 - ¹¹ Department of Automatic Control and Robotics, Faculty of Electrical Engineering, Automatics, Computer 22 Science and Biomedical Engineering, AGH University of Science and Technology, A. Mickiewicza 30, 23-059 Kraków, Poland; adglow@agh.edu.pl
- * Correspondence: usmanillahi83@gmail.com (U.I.); fazal.muhammad@uetmardan.edu.pk (F.M.)



Citation: Illahi, U.; Iqbal, J.; Irfan, M.; Ismail Sulaiman, M.; Khan, M.A.; Rauf, A.; Bari, I.; Abdullah, M.; Muhammad, F.; Nowakowski, G.; et al. A Novel Design and Development of a Strip-Fed Circularly Polarized Rectangular Dielectric Resonator Antenna for 5G NR Sub-6 GHz Band Applications. *Sensors* **2022**, *22*, 5531. <https://doi.org/10.3390/s22155531>

Academic Editors: Tiago Varum and Joao Nuno Matos

Received: 7 June 2022

Accepted: 22 July 2022

Published: 25 July 2022

Publisher's Note: MDPI stays neutral with regard to jurisdictional claims in published maps and institutional affiliations.



Copyright: © 2022 by the authors. Licensee MDPI, Basel, Switzerland. This article is an open access article distributed under the terms and conditions of the Creative Commons Attribution (CC BY) license (<https://creativecommons.org/licenses/by/4.0/>).

Abstract: In this article, a rectangular dielectric resonator antenna (RDRA) with circularly polarized (CP) response is presented for 5G NR (New Radio) Sub-6 GHz band applications. A uniquely shaped conformal metal feeding strip is proposed to excite the RDRA in higher-order mode for high gain utilization. By using the proposed feeding mechanism, the degenerate mode pair of the first higher-order, i.e., $TE_{\delta 13}^x$ at 4.13 GHz and $TE_{1\delta 3}^y$ at 4.52 GHz is excited to achieve a circularly polarized response. A circular polarization over a bandwidth of ~10%, in conjunction with a wide impedance matching over a bandwidth of ~17%, were attained by the antenna. The CP antenna proposed offers a useful gain of ~6.2 dBi. The achieved CP bandwidth of the RDRA is good enough to cover the targeted 5G NR bands around 4.4–4.8 GHz, such as n79. The proposed antenna configuration is modelled and optimized using computer simulation technology (CST). A prototype was built to confirm (validate) the performance estimated through simulation. A good agreement was observed between simulated and measured results.

Keywords: dielectric resonator antennas; strip-fed antennas; axial ratio; 5G NR band; Sub-6 GHz

1. Introduction

The 5G New Radio (NR) is a newly developed air interface to fulfill the requirements of modern communications. 5G wireless technology is becoming popular because of its significant features, such as high data rate, low latency response time, and high bandwidth [1].

The 5G NR is a multi-band spectrum and n79 (4.4–4.8 GHz) is one of the major focuses for future 5G communications in different parts of the world, such as China, the EU, and Japan [2]. In literature, different 5G antennas have been reported so far [3,4]. In the last few decades, the dielectric resonator antenna (DRA) has been acquiring a lot of attention from antenna researchers. This is due to their significant benefits over conventional microstrip antennas. DRAs offer high bandwidth, negligible metal losses, small size, and fixable excitation techniques which make them a potential candidate for high-frequency modern networks, such as 5G [5–12].

DRAs can be designed in different shapes for desired applications but complicated shapes add complexity and design configurations are expensive. So basic dielectric resonator (DR) shapes, such as rectangular, cylindrical, and hemispherical are much more popular because of ease in fabrication and low cost. Among these basic shapes, rectangular is much preferred because of design flexibility. In the rectangular shape, the height to width and depth to width aspect ratios have a direct impact on resonance frequency and Q-factor of the radiation. Moreover, using the dielectric waveguide model (DWM), the DR profile and impedance bandwidth characteristics of the rectangular DRA can be predicted [13].

In this era of modern communication, reliability of the communication system is highly important. That is why circularly polarized communication networks are very much preferred as compared to linearly polarized communication networks [3]. A lot of circularly polarized DRAs are reported in the literature using dual feeding techniques, but with limitations, such as complex feeding networks and larger sizes, which make them useless for modern communication [14–16]. The generation of circular polarization in DRA using a single feeding network is quite challenging. Some authors performed cutting and drilling of the dielectric resonator, some used multi-layered DRs, having metallic walls surrounding the RDRA, and more than one DR has been reported as well. All such arrangements are complex, heavy, and costly [17–20].

Different DRAs using a single feeding mechanism have been reported in the literature [18–22]. In [18], a multi-layered rectangular DRA, excited by a cross-slot coupled with a microstrip feeding mechanism providing 9.5% of CP response, has been reported. As demonstrated in [19], a feeding technique comprised of cross-slot and microstrip was used to generate a 46.9% CP wave by a rectangular DRA surrounded by four metallic walls. As presented by M. Elahi et al., in [20], a 3 dB axial ratio bandwidth of 5.5% was attained by using two annular vias (holes) in a rectangular DR excited by a rectangular slot coupled microstrip line feed. As reported by A. Gupta et al., in [21], the CP bandwidth of 2.29% is achieved using rectangular DR excited by a triangular ring-shaped aperture with a parasitic patch. A cross-slot coupled with a microstrip line to attain CP bandwidth of 2.2% using rectangular-shaped DR was reported in [22]. In all discussed literature a sufficient bandwidth of impedance matching was achieved to cover the attained AR bandwidth. However, it is clarified that the generation of circular polarization using a single feeding mechanism with simple design geometry is quite challenging and a solution to this problem is reported in this article.

In this research paper, a new feeding mechanism, using a uniquely shaped conformal metal strip, is introduced to excite the rectangular DRA for CP response. The proposed feeding technique excites the degenerate higher-order mode pair to generate the circularly polarized wave. A prototype was built to study the experimental results. Antenna parameters, such as impedance matching, axial ratio, beamwidth, and gain, were studied theoretically and experimentally. A reasonable similarity was observed in all antenna parameters. The proposed antenna could be used for 5G Sub-6 GHz communications around 4.4–4.8 GHz, such as n79 [2]. In Section 2, antenna design geometry is explained. In Section 3, antenna design, optimization, and CP generation mechanism are discussed in detail. In Section 4 comparison between experiment and theory is demonstrated and explained. Section 5 features the conclusion to the article.

2. Antenna Geometry

Figure 1 presents the configuration of the proposed geometry of the circularly polarized antenna excited by a uniquely shaped conformal strip placed with a feed point at the central position. The design was modeled in CST[®] Microwave Studio using its time domain-based finite integration technique [23]. Hexahedral meshing was used to design a rectangular DRA with DR permittivity, $\epsilon_r = 10$ [11]. In settings, the cell per wavelength was set at a value of 40 and the cells per max model box edge at 20 for design meshing. The fraction of maximum cell near to model was also set at a value of 20 and total unknowns of 559,980 were obtained.

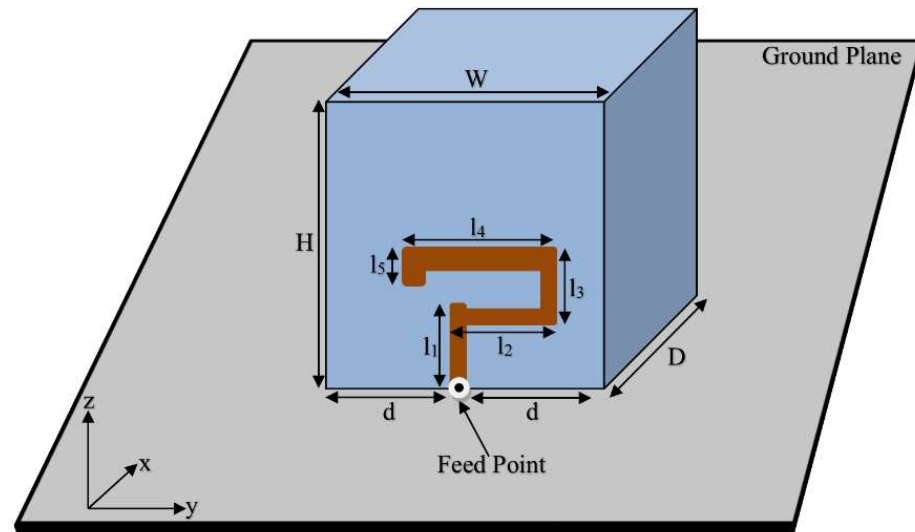


Figure 1. The geometry of the proposed CP 5G RDRA.

An iterative design procedure was followed to determine the optimum dimensions of the feeding metallic strips that were needed to excite the degenerate TE_{813}^x and TE_{163}^y necessary for CP wave generation [24]. The DR profile dimensions of $H = 26.1$ mm, $W = 25.4$ mm, and $D = 14.3$ mm were used. The optimization of the lengths and the widths of the strip were performed by running different simulations using many parameter sweeps. The results of the design procedure are summarized in Table 1, which shows several selected dimensions of l_1 , l_2 , l_3 , l_4 , and l_5 that could generate circular polarization in conjunction with sufficient impedance matching bandwidth.

Table 1. AR and S_{11} bandwidths for different feed dimensions of the proposed CP 5G RDRA.

l_1 (mm)	l_2 (mm)	l_3 (mm)	l_4 (mm)	l_5 (mm)	3 dB AR Bandwidth (%)	10 dB S_{11} Bandwidth (%)	Overlapping AR & S_{11} Bandwidth (%)
3.5	7	1	8	1	6.24	12.43	100
		2	8	0.5	5.65	12.18	100
				0.5	6.23	11.92	100
	9	2	12	1	6.64	10.65	100
				1	7.87	10.4	100
				2.5	6.17	10.14	93.1
			3	7.08	11.67	76.2	
			1.5	9.07	11.42	66.2	

Table 1. Cont.

l_1 (mm)	l_2 (mm)	l_3 (mm)	l_4 (mm)	l_5 (mm)	3 dB AR Bandwidth (%)	10 dB S11 Bandwidth (%)	Overlapping AR & S11 Bandwidth (%)		
3.5		3	10	2.5	5.64	11.16	90.5		
				3	6.28	8.63	86.3		
				2	7.25	8.38	100		
5.5	7	3	7	1.5	4.17	9.89	100		
				1	5.32	9.63	100		
				2.5	7.59	9.38	100		
		4	8	3.5	7.43	9.13	100		
		5	10	1.5	10	17	100		
		9	5	12	2	5.07	7.9	48.3	
7.5		5	6	5	8	4	6.15	7.42	77.5
				3.5	4.71	7.2	100		
				2.5	7.08	6.97	43.4		
		7	7	8	2	6.15	6.75	100	
					2	6.1	6.54	100	
		9	6	10	3	1.5	5.3	6.34	100
						3.5	10.47	10.91	60.3
9	6	10	3	4.05	7.66	100			

3. Circularly Polarized 5G Antenna Design and Optimization

In this section, the design and development of CP 5G NR Sub-6 GHz RDRA are explained in detail. Moreover, the antenna optimization, along with results, is discussed. The lengths and widths of the feeding strip were very critical in this design configuration which is herein demonstrated and discussed. It is a well-known fact that a circularly polarized wave can be generated if the feeding network is capable of exciting the orthogonal degenerate modes, since such excitation generates two far-field components that are equal in magnitude with the quadrature phase shift necessary for CP generation [25]. In this section an initially linearly polarized rectangular DRA was designed using a single conformal strip. The next feeding mechanism was modified step by step to design a circularly polarized DRA without adding any complicated changes. Five different design geometries for the development of CP 5G Sub-6 GHz RDRA are presented and discussed in detail.

3.1. Geometry 1

In Figure 2a geometry 1 of RDRA is depicted. As shown, the antenna was designed by placing a single conformal strip at the middle of the surface of the DRA. The antenna was linearly polarized because such excitation does not excite the degenerate mode. Only TE_{183}^y was energized, at around 4.47 GHz, to generate a linearly polarized wave, as shown in Figure 3. The result of the axial ratio of geometry 1 is not shown in Figure 4.

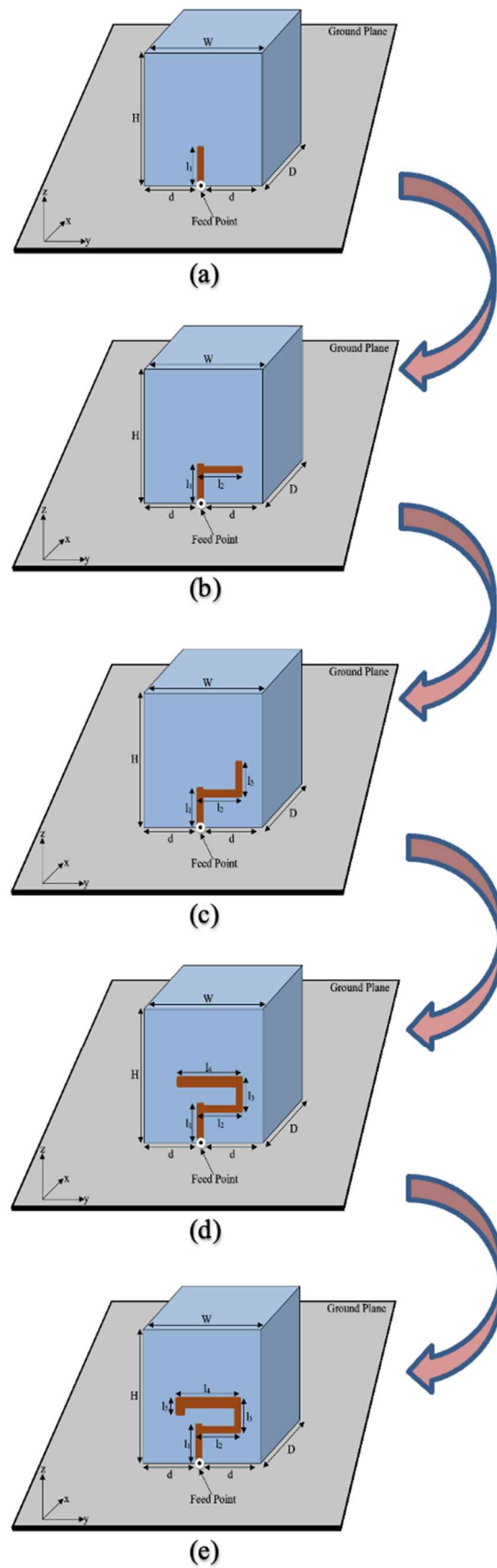


Figure 2. Step by step development of the CP 5G RDRA. (a) Geometry 1; (b) Geometry 2; (c) Geometry 3; (d) Geometry 4; (e) Geometry of the Proposed CP 5G RDRA.

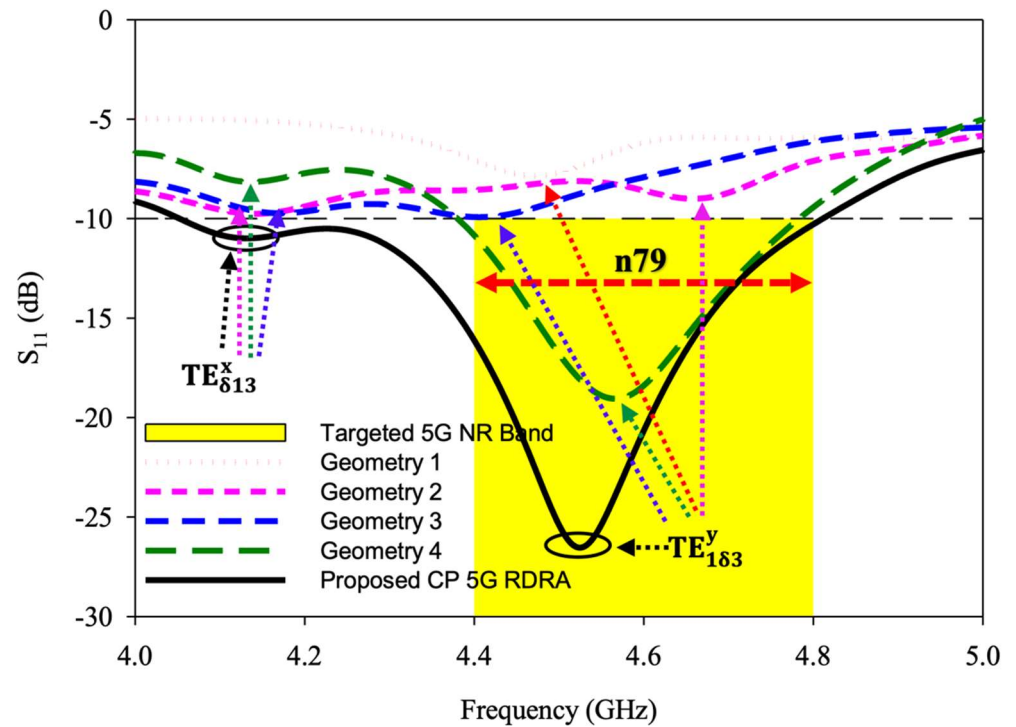


Figure 3. Return losses comparison of different geometries toward the development of the CP 5G RDRA.

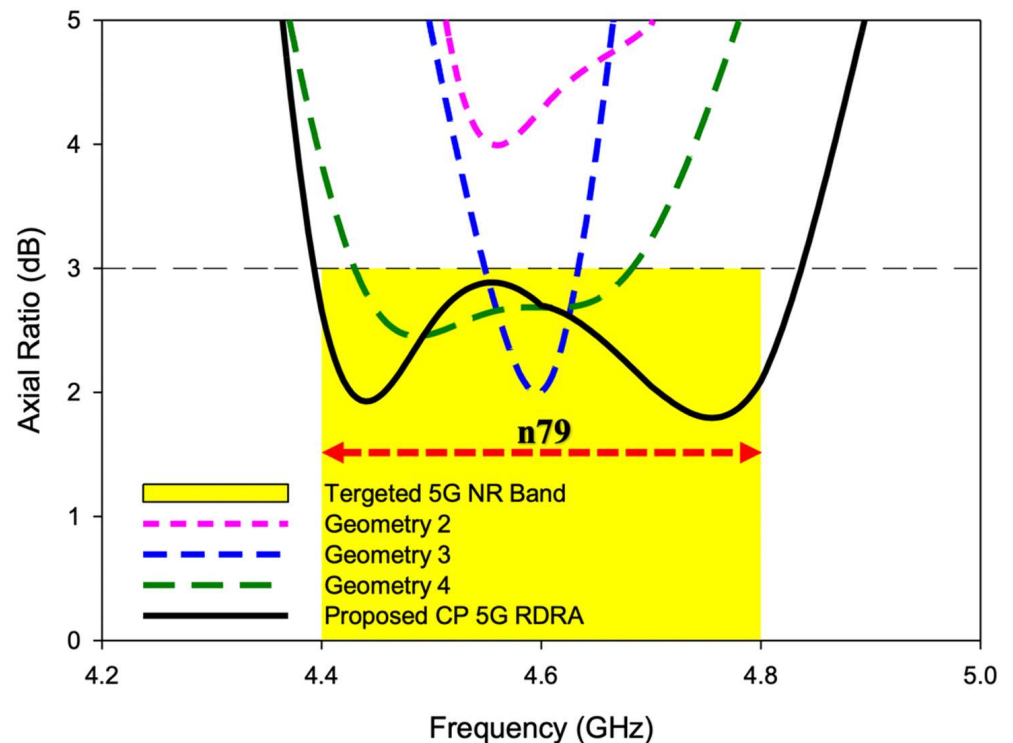


Figure 4. Axial ratios comparison of different geometries toward the development of the CP 5G RDRA.

3.2. Geometry 2

The geometry 2 of RDRA is shown in Figure 2b. The feeding strip was modified by adding one more length. Using this configuration, the RDRA showed behavior towards CP

response. The degenerate mode was excited but still, S_{11} bandwidth below -10 dB was nil, as shown in Figure 3. As presented in Figure 3, the degenerate mode pair of the first higher-order, i.e., $TE_{\delta 13}^x$ and $TE_{1\delta 3}^y$, was excited at 4.12 GHz and 4.66 GHz, respectively. The CP response of the antenna is depicted in Figure 4, and, as shown, the 3-dB axial ratio bandwidth was nil as well. The results of this configuration were encouraging, but needed further modification and optimization to achieve the desired bandwidths for the targeted application. Geometry 2 was further modified, and the impact of the modification is discussed in the next section.

3.3. Geometry 3

In geometry 3 the RDRA was energized by adding one more strip, as presented in Figure 2c. The modification is discussed in the next section. The return losses of this design configuration are depicted in Figure 3. The S_{11} curve of geometry 3 shows that the degenerate $TE_{\delta 13}^x$ was excited at 4.16 GHz and $TE_{1\delta 3}^y$ at 4.4 GHz, but still, impedance matching ($|S_{11}| \leq 10$ dB) was not achieved. As shown in Figure 4, the 3 dB axial ratio bandwidth of $\sim 2\%$ was achieved. The provided bandwidth was not enough to cover the targeted 5G band. Moreover, the S_{11} of the antenna needed to be optimized further. So, the shape of the feeding strip was further changed and this is discussed in the next geometry.

3.4. Geometry 4

The geometry 4 of RDRA is presented in Figure 2d. This design configuration was achieved by adding an additional length to the feeding strip. At this stage, the feeding strip was composed of 4 different lengths. The impedance matching ($|S_{11}| \leq 10$ dB) over a bandwidth of $\sim 8.8\%$ was attained by this configuration, as shown in Figure 3. The degenerate mode pair of the first higher-order, i.e., $TE_{\delta 13}^x$ at 4.14 GHz and $TE_{1\delta 3}^y$, at 4.55 GHz was excited to generate the circularly polarized response. The circular polarization over a bandwidth of $\sim 5.8\%$ was provided by the antenna. A significant improvement was observed in S_{11} and AR ratio bandwidths but, still, the achieved CP response was not enough to cover the desired bandwidth i.e., 4.4–4.8 GHz. This design configuration was again modified to make the final proposed geometry.

3.5. Geometry of the Proposed CP 5G RDRA

The final design geometry was developed by adding the fifth and last length to the feeding strip to make the desired 5G Sub-6 GHz rectangular DRA, as depicted in Figures 1 and 2b. The optimized strip lengths were $l_1 = 5.5$ mm, $l_2 = 7$ mm, $l_3 = 5$ mm, $l_4 = 10$ mm, and $l_5 = 1.5$ mm. The feed parameters were optimized by running a number of simulation sweeps to get the desired CP response. An impedance matching ($|S_{11}| \leq 10$ dB) over a bandwidth of $\sim 17\%$ was provided by the proposed geometry, as presented in Figure 3. As shown, the degenerate modes $TE_{\delta 13}^x$ at 4.13 GHz and $TE_{1\delta 3}^y$ at 4.52 GHz were excited to generate the circularly polarized response. The E-field and H-field distribution of the proposed CP 5G RDRA are depicted in Figures 5 and 6, respectively.

The CP response over a bandwidth of $\sim 10\%$ was provided by the antenna. The achieved 3 dB axial ratio extended from 4.4–4.84 GHz which was good enough to cover the targeted n79 band. The AR and S_{11} bandwidths were achieved over the same range, as shown in Figure 7. Moreover, as the DRA radiated away from the ground the size did affect the performance much [26]. The antenna was simulated on different ground plane sizes and the results of S_{11} and the axial ratio are presented in Figures 8 and 9. The simulated surface current distributions of the antenna at 4.13 GHz (Minimum of S_{11}) are depicted in Figure 10. As can be seen the composite current surface currents on the novel feed were orthogonal at 0° and 90° , which provided the required condition for CP generation.

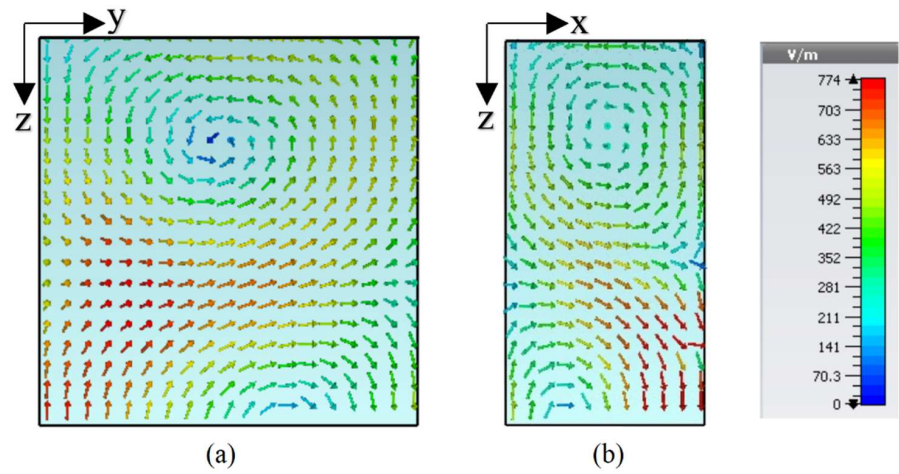


Figure 5. E-field distribution of the CP 5G RDRA (a) $TE_{\delta 13}^x$ at 4.13 GHz; (b) $TE_{1\delta 3}^y$ at 4.52 GHz.

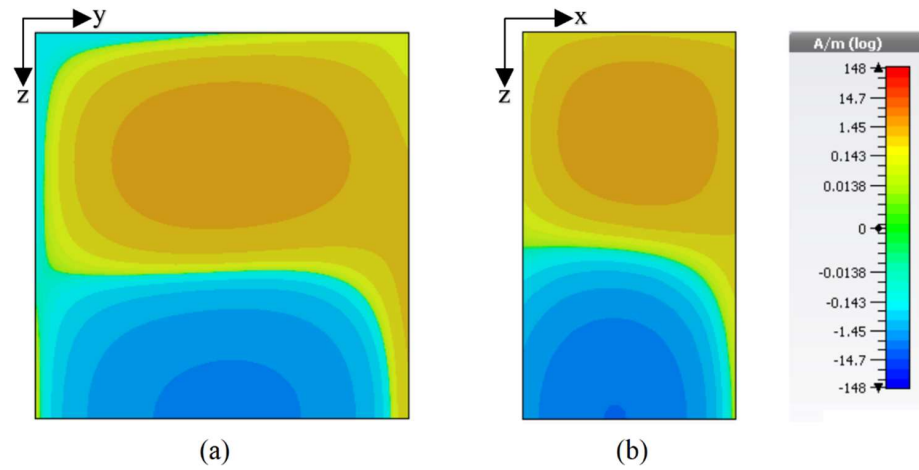


Figure 6. H-field distribution of the CP 5G RDRA (a) $TE_{\delta 13}^x$ at 4.13 GHz; (b) $TE_{1\delta 3}^y$ at 4.52 GHz.

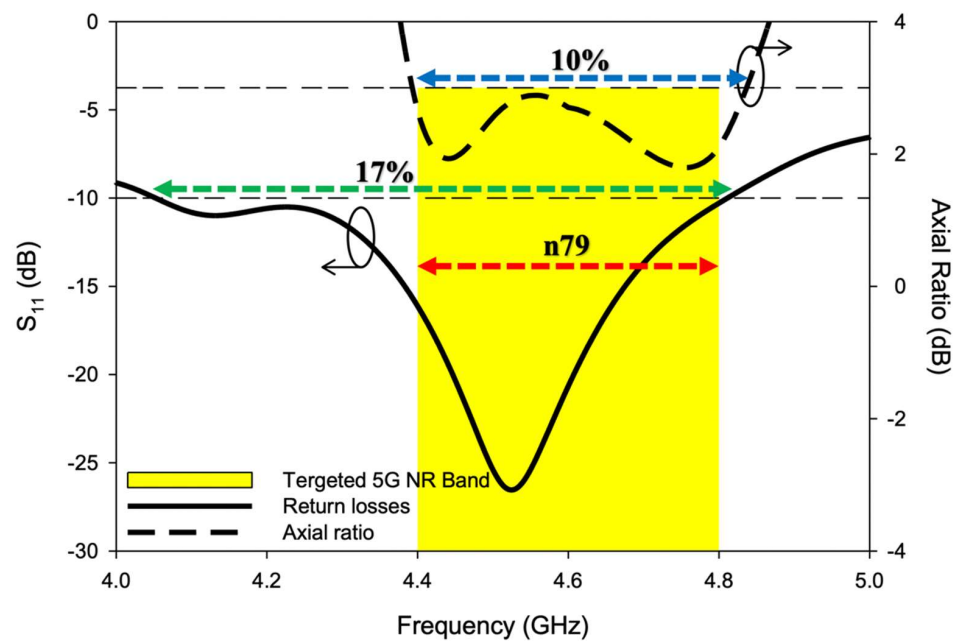


Figure 7. S_{11} and AR ratio overlapping bandwidths of the CP 5G RDRA.

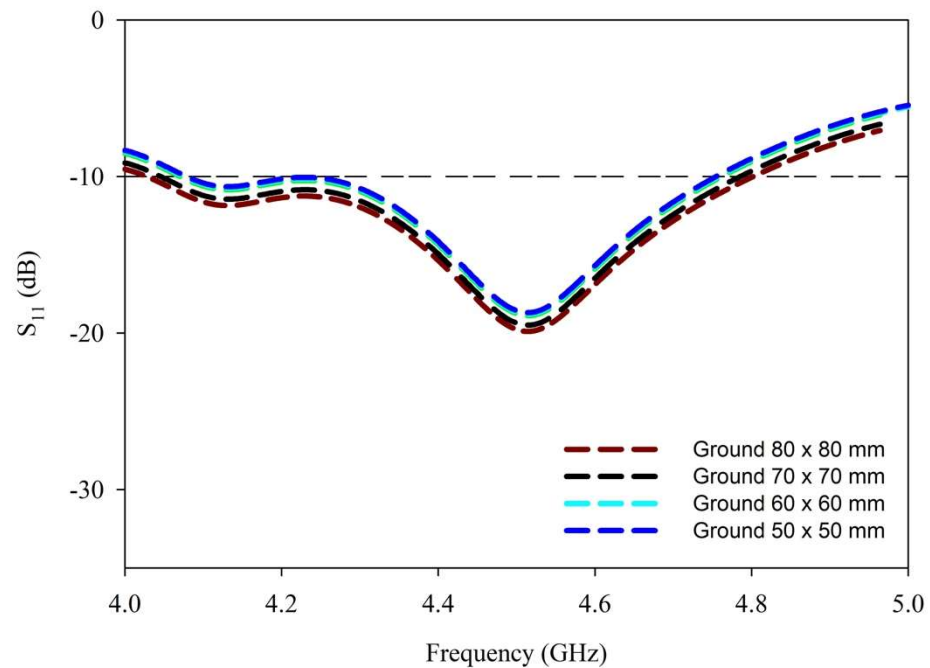


Figure 8. S₁₁ of the CP 5G RDRA with different ground plane sizes.

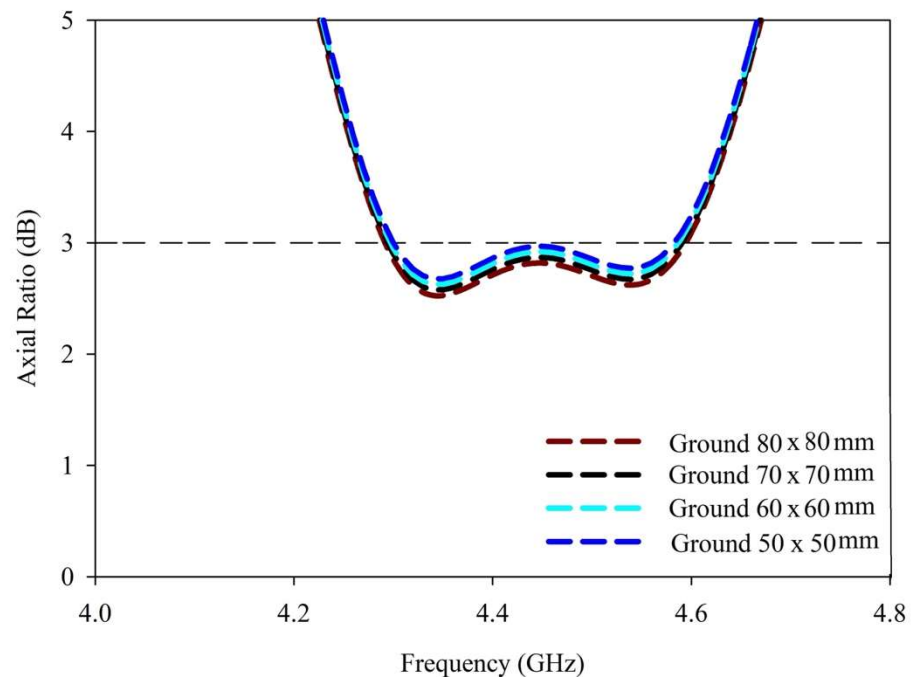


Figure 9. AR ratio of the CP 5G RDR with different ground plane sizes.

The wideband CP response and higher-order mode excitation were achieved using a low-cost simple design configuration without any complexity, which is a good contribution to those reported in the literature. The performance comparison of different geometries in the development of the desired CP 5G Sub-6 GHz antenna is summarized in Table 2. The optimized circularly polarized antenna was then fabricated to experimentally validate the proposed design which is demonstrated and explained in the next section.

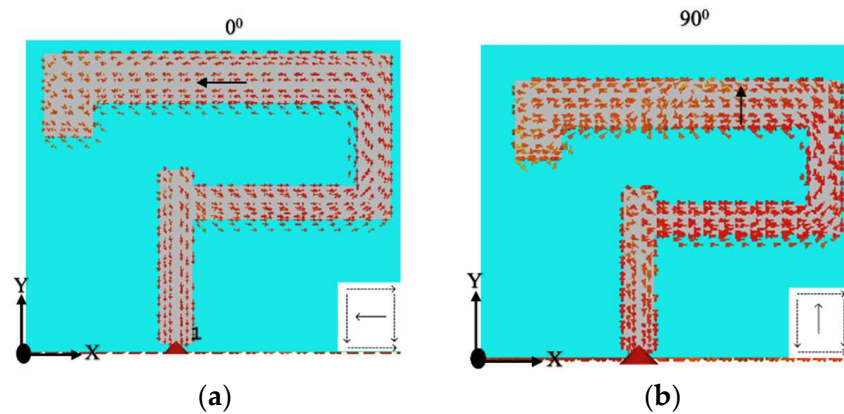
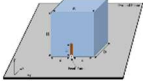
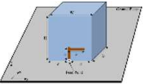
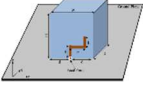
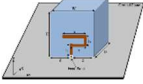
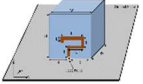


Figure 10. The surface current distribution at the novel feed of the CP 5G RDR. (a) At 0° ; (b) At 90° .

Table 2. Performance comparison of different geometries in the development of the CP 5G RDRA.

Antenna	Geometry	No of Strips	10-dB S_{11} Bandwidth (%)	3-dB AR Bandwidth (%)	Polarization	5G NR n79 Coverage (4.4–4.8 GHz)
Geometry 1		1	Nil	Nil	Linear	NO
Geometry 2		2	Nil	Nil	Circular	NO
Geometry 3		3	Nil	2	Circular	NO
Geometry 4		4	8.8	5.8	Circular	NO
Proposed CP 5G RDRA		5	17	10	Circular	YES

4. Measurement Results

The optimized 5G NR band circularly polarized antenna was finally fabricated to measure the experimental results. The photographs of the proposed prototype are presented in Figure 11. The closeup, front view, top view, and back view of the antenna are depicted in Figure 11a–d, respectively. The ECCOSTOCK HiK with permittivity, $\epsilon_r = 10$ having loss tangent (δ) of 0.002 was used as DR material. An 80×80 mm aluminum ground plane was used. The feeding strip was cut from adhesive copper tape to easily stick to the surface of the DRA. An SMA was soldered at the feed point at the center of the DRA with the feeding strip. S_{11} was measured using a vector network analyzer (VNA), while far-field parameters were measured in the anechoic chamber. A $50\text{-}\Omega$ coaxial cable was used to connect the SMA with the VNA. Double-sided copper tape was used to stick the DRA on the aluminum ground plane] to remove the possible air gap, according to the procedure explained in [26].

The resonant mode frequencies of the RDRA could be predicted using mathematical equations of the dielectric waveguide model, as explained in [27]. According to DWM $TE_{\delta 13}^x$ was estimated at 3.89 GHz and $TE_{1\delta 1}^y$ at 4.53 GHz. The comparison between simulated and measured S_{11} of the CP DRA is presented in Figure 12. $TE_{\delta 13}^x$ was simulated at 4.13 GHz and measured at 4.12 GHz while $TE_{1\delta 3}^y$ was simulated at 4.52 GHz and measured at 4.51 GHz. A close comparison was observed between predicted, simulated, and measured values.

The comparison of these values is presented ed in Table 3. The impedance matching bandwidth ($|S_{11}| \leq 10$ dB) expanded from 4.05–4.81 GHz in simulation and 4.01–4.83 GHz in measurement. The antenna provided a measured S_{11} over a bandwidth of ~17%. A small marginal difference between simulation and measurement was observed, due to cable losses and measurement errors.

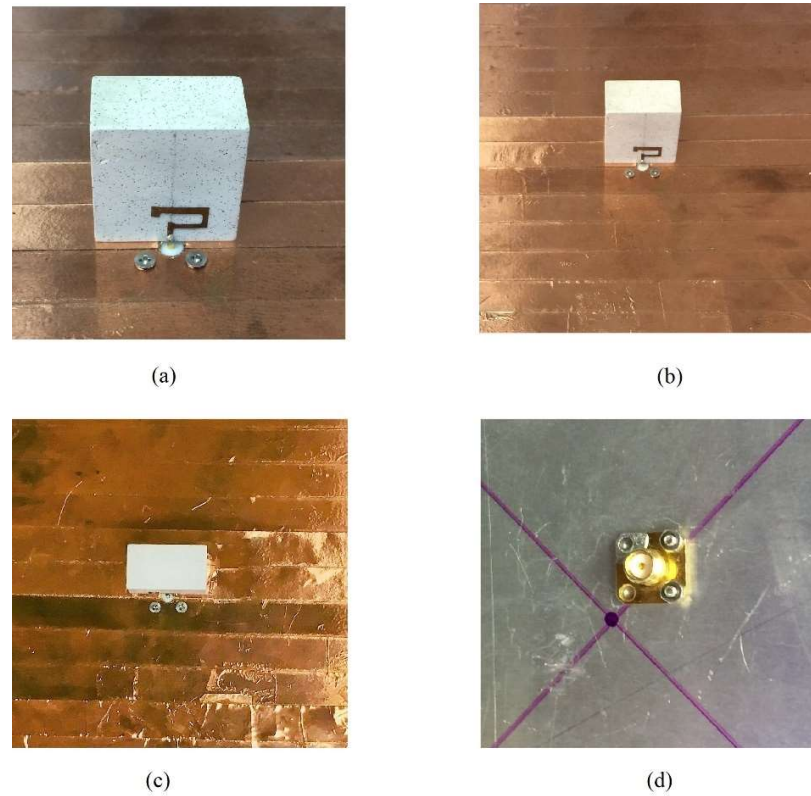


Figure 11. The geometry of the Proposed CP 5G RDRA Photograph of the prototype of the CP 5G RDRA. (a) Closeup; (b) Front View; (c) Top view; (d) Back view.

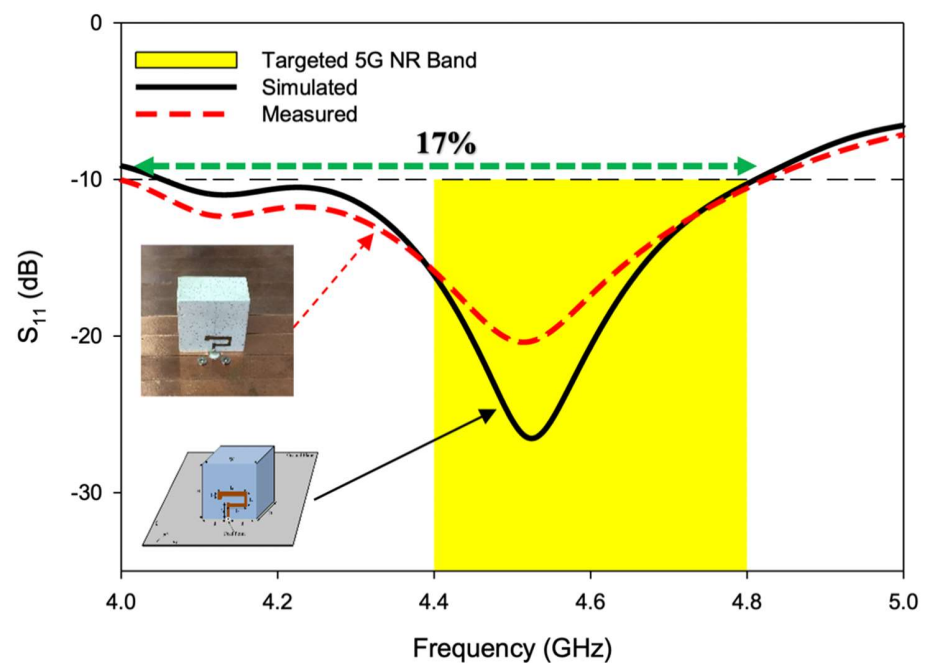
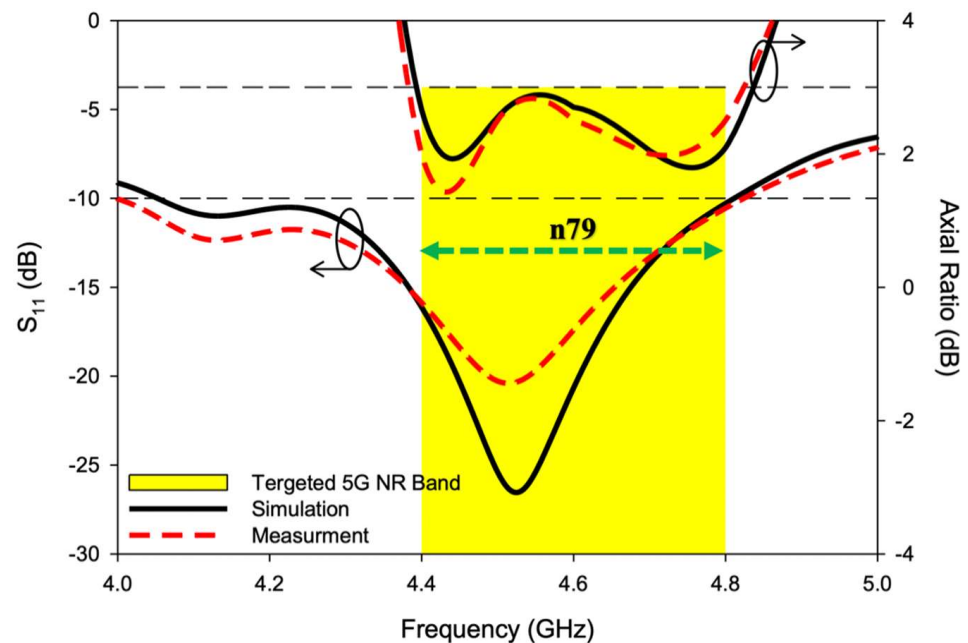


Figure 12. Simulated and measured S_{11} of the CP 5G RDRA.

Table 3. Comparison between predicted, simulated, and measured mode frequencies of the CP 5G RDRA.

Excited Mode of 5G CP RDRA	DWM Estimation	CST Calculation	Experimental Measurement
TE	f_{DWM} (GHz)	f_{CST} (GHz)	$f_{Measurement}$ (GHz)
TE_{813}^x	3.89	4.13	4.12
TE_{183}^y	4.53	4.52	4.51

Figure 13 shows the simulated and measured CP response of the proposed RDRA in the boresight direction (i.e., $\theta = 0^\circ$, $\Phi = 0^\circ$). As presented, the axial ratio extended from 4.4–4.84 GHz in simulation, while 4.38–4.82 GHz was measured during the experiment. Circular polarization of bandwidth of $\sim 10\%$ was achieved, both in simulation and measurement. The minimum AR value was simulated at 4.44 GHz and measured at 4.43 GHz with a magnitude of 1.92 dB and 1.4 dB, respectively. The negligible difference between theory and experiment was due to cable losses and measurement imperfections. The successful overlap of S11 and AR bandwidths is depicted in Figure 14. As shown, the overlapped bandwidth was good enough to cover the targeted 5G NR Sub-6 GHz band i.e., n79 (4.4–4.8 GHz). A stable and satisfactory performance was offered by the antenna during the experiment.

**Figure 13.** Simulated and measured axial ratio of the CP 5G RDRA.

The simulated and measured radiation patterns of the proposed CP 5G RDRA are presented in Figure 15. The radiation patterns were computed and measured at three different frequencies. The antenna provided stable radiation patterns with left-hand circular polarization, since the left-hand field component was greater than the right-hand field component by a margin of more than 20 dB at minimum AR frequency i.e., 4.43 GHz, as shown in Figure 15b. The right-hand CP response could be achieved by reversing the feeding strip. The simulated and measured gain of the CP antenna are shown in Figure 16. The antenna offers a useful gain of ~ 6.2 dBic throughout the CP bandwidth. This high gain was achieved by excitation of the higher-order mode. A reasonable resemblance was observed between simulated and measured results.

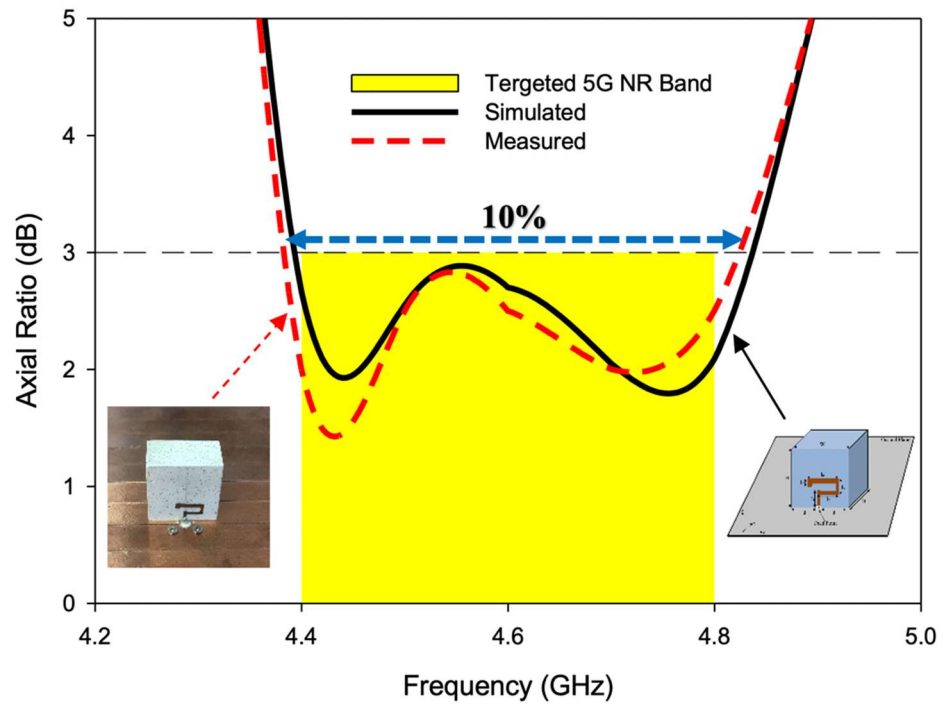


Figure 14. Simulated and measured S_{11} and AR overlapping bandwidths of the CP 5G RDRA.

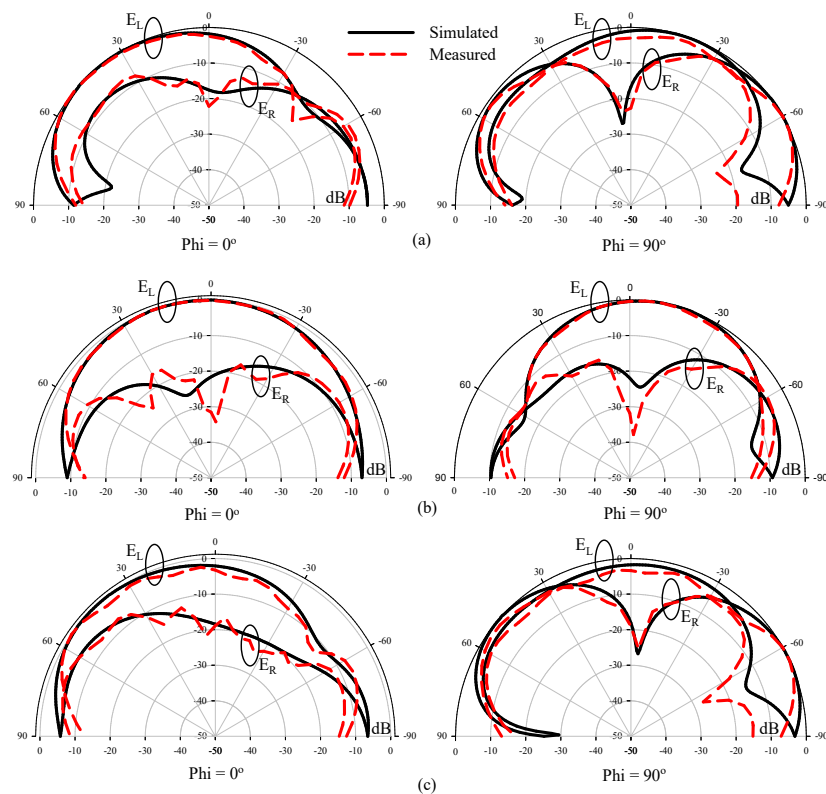


Figure 15. Simulated and measured radiation patterns of the CP 5G RDRA. (a) 4.4 GHz; (b) 4.43 GHz; (c) 4.7 GHz.

In Table 4, the proposed CP 5G RDRA is compared with recently reported RDRAs in the literature. It can be concluded that the proposed design configuration offers wide CP bandwidth achieved by excitation of the orthogonal higher-order mode pair, with

very simple design geometry. Basic DR shape, i.e., rectangular, was used as radiating element along with the implementation of a simple feeding mechanism. Moreover, the field distribution inside the DRA was controlled by short adjacent magnetic dipoles. The spacing between these dipoles was responsible for the gain of the DRA, which could be improved by increasing the spacing. The spacing could be enhanced by excitation of the DRA in higher-order mode [28]. In literature, different efforts have been made to excite the RDRA in higher-order mode for high gain applications but the reported geometries are complicated and not easy to implement. In the proposed antenna higher-order orthogonal mode was excited using a new conformal feeding strip that was cut from an adhesive copper tape, which is a simple and cost-effective solution to the problem.

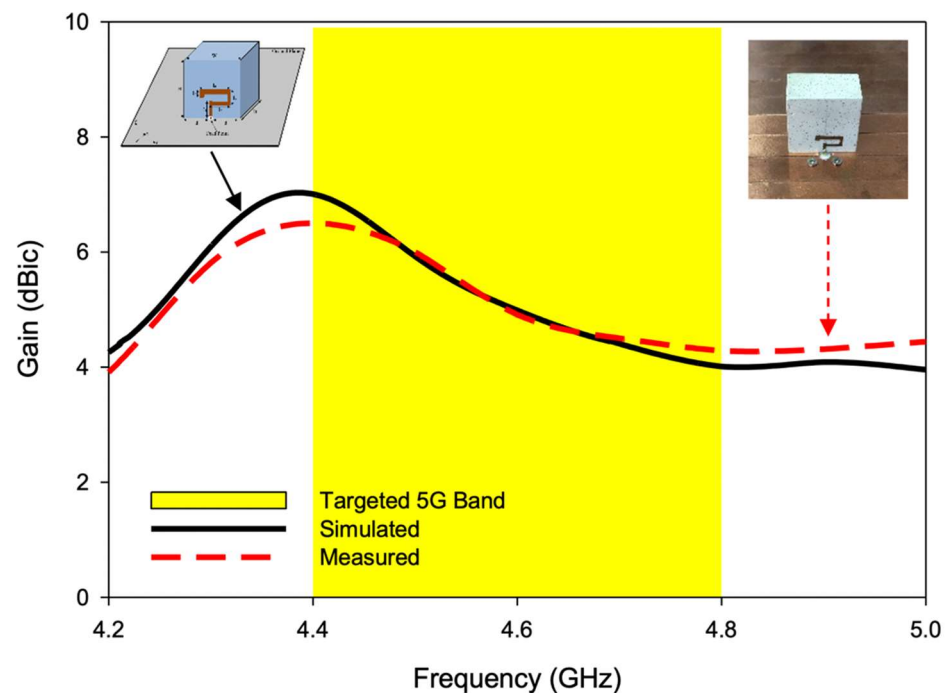


Figure 16. Simulated and measured gain of the CP 5G RDRA.

Table 4. Comparison between proposed CP 5G RDRA with recently reported RDRA in literature.

Ref.	ϵ_r	Design Configuration	Excitation Mechanism	Mode of Excitation	Usable CP Frequency	Usable CP Bandwidth	Gain (dBic)	Antenna Geometry
[18]	10 & 3.5	Rectangular multilayered DRA	Cross-slot with microstrip line	TE ₁₁₁ & TE ₁₁₃	10.5–11.5 GHz	9.5%	11	Complex
[19]	10	Four metallic walls surrounded RDRA	Cross-slot with microstrip line	TE ₁₁₁	2.2–3.5 GHz	46.9%	4.37	Complex
[20]	9.6	Rectangular DRA with two annular vias	Microstrip line coupled rectangular slot	TE ₁₁₃	3.28–3.46 GHz	5.5%	6–7.1	Complex
[21]	9.8	Rectangular DRA	Triangular aperture with parasitic strip	TE ₁₁₁	3.46–3.54 GHz	2.29%	5	Complex
[22]	20.5	Rectangular DRA	Cross-slot-coupled	TE ₁₁₁	1.25–1.3 GHz	2.2%	4.3	Complex
Proposed CP 5G RDRA	10	Rectangular DRA	Unique conformal strip	TE ₁₁₃	4.4–4.8 GHz	10%	6.2	Simple

5. Conclusions

This paper reported on a new low-cost circularly polarized RDRA for 5G NR Sub-6 GHz band applications. A new conformal metal strip was utilized for excitation of the higher-order orthogonal mode pair to generate CP response. A circular polarization over a bandwidth of ~10% was achieved along with a wide impedance matching bandwidth of ~17%. The axial ratio bandwidth was in conjunction with impedance matching bandwidth. A left-hand CP response was achieved with stable radiation patterns throughout the circular polarization bandwidth. A useful gain of ~6.2 dBic was attained by the antenna. The use of a simple and low-cost feeding mechanism, i.e., a unique conformal strip, to generate a circularly polarized wave by excitation of higher-order orthogonal modes, is the significant feature of this research, as compared to reports in the literature. A good agreement was observed in simulation and experimental results.

Author Contributions: Conceptualization, U.I., A.R. and J.I.; methodology, U.I. and J.I.; software, U.I., I.B. and F.M.; validation, M.A.K., I.B. and F.M.; formal analysis, M.A.K., I.B. and F.M.; investigation, M.A. and M.I.S.; resources, M.A., M.I.S. and F.M.; data curation, A.R. and J.I.; writing—original draft preparation, U.I. and J.I.; writing—review and editing, M.I., A.G. and G.N.; visualization M.I., A.G. and G.N.; supervision, M.I., A.G. and U.I.; project administration, M.I., M.A. and G.N.; funding acquisition, M.I., A.G., M.A.K. and A.R. All authors have read and agreed to the published version of the manuscript.

Funding: The APC of the journal was supported by the Faculty of Electrical and Computer Engineering, Cracow University of Technology and by the Ministry of Science and Higher Education, Republic of Poland (grant No. E-1/2022).

Institutional Review Board Statement: Not applicable.

Informed Consent Statement: Not applicable.

Data Availability Statement: All data has been included in the study.

Acknowledgments: The authors acknowledge the support from the Deanship of Scientific Research, Najran University, Kingdom of Saudi Arabia.

Conflicts of Interest: The authors declare no conflict of interest.

References

1. Rafique, U.; Khan, S.; Ahmed, M.M.; Kiani, S.H.; Abbas, S.M.; Saeed, S.I.; Alibakhshikenari, M.; Dalarsson, M. Uni-Planar MIMO Antenna for Sub-6 GHz 5G Mobile Phone Applications. *Appl. Sci.* **2022**, *12*, 3746. [[CrossRef](#)]
2. Kiani, S.H.; Iqbal, A.; Wong, S.W.; Savci, H.S.; Alibakhshikenari, M.; Dalarsson, M. Multiple Elements MIMO Antenna System with Broadband Operation for 5th Generation Smart Phones. *IEEE Access* **2022**, *10*, 38446–38457. [[CrossRef](#)]
3. Illahi, U.; Iqbal, J.; Sulaiman, M.I.; Alam, M.; Su'ud, M.M.; Khattak, M.I. Design and development of a singly-fed circularly polarized rectangular dielectric resonator antenna for WiMAX/Satellite/5G NR band applications. *AEU Int. J. Electron. Commun.* **2020**, *126*, 153443. [[CrossRef](#)]
4. Chen, H.N.; Song, J.; Park, J. A Compact Circularly Polarized MIMO Dielectric Resonator Antenna over Electromagnetic Band-Gap Surface for 5G Applications. *IEEE Access* **2019**, *7*, 140889–140898. [[CrossRef](#)]
5. Mukherjee, B.; Patel, P.; Mukherjee, J. A review of the recent advances in dielectric resonator antennas. *J. Electromagn. Waves Appl.* **2020**, *34*, 1095–1158. [[CrossRef](#)]
6. Ahmad, Z.; Hesselbarth, J. On-Chip Dual-Polarized Dielectric Resonator Antenna for Millimeter-Wave Applications. *IEEE Antennas Wirel. Propag. Lett.* **2018**, *17*, 1769–1772. [[CrossRef](#)]
7. Baldazzi, E.; Al-Rawi, A.; Cicchetti, R.; Smolders, A.B.; Testa, O.; van Coevorden Moreno, C.D.; Caratelli, D. A High-Gain Dielectric Resonator Antenna with Plastic-Based Conical Horn for Millimeter-Wave Applications. *IEEE Antennas Wirel. Propag. Lett.* **2020**, *19*, 949–953. [[CrossRef](#)]
8. Mishra, N.K.; Das, S.; Vishwakarma, D.K. Beam steered linear array of cylindrical dielectric resonator antenna. *AEU-Int. J. Electron. Commun.* **2019**, *98*, 106–113. [[CrossRef](#)]
9. Anuar, S.U.; Jamaluddin, M.H.; Din, J.; Kamardin, K.; Dahri, M.H.; Idris, I.H. Triple band mimo dielectric resonator antenna for lte applications. *AEU-Int. J. Electron. Commun.* **2020**, *118*, 153172. [[CrossRef](#)]
10. Mazhar, W.; Klymyshyn, D.M.; Wells, G.; Qureshi, A.A.; Jacobs, M.; Achenbach, S. Low-Profile Artificial Grid Dielectric Resonator Antenna Arrays for mm-Wave Applications. *IEEE Trans. Antennas Propag.* **2019**, *67*, 4406–4417. [[CrossRef](#)]

11. Iqbal, J.; Illahi, U.; Yasin, M.N.M.; Albreem, M.A.; Akbar, F.M. Bandwidth enhancement by using parasitic patch on dielectric resonator antenna for sub-6 GHz 5G NR bands application. *Alex. Eng. J.* **2022**, *61*, 5021–5032. [[CrossRef](#)]
12. Boyuan, M.; Pan, J.; Wang, E.; Yang, D. Wristwatch-Style Wearable Dielectric Resonator Antennas for Applications on Limbs. *IEEE Access* **2020**, *8*, 59837–59844. [[CrossRef](#)]
13. Mongia, R.K.; Ittipiboon, A. Theoretical and experimental investigations on rectangular dielectric resonator antennas. *IEEE Trans. Antennas Propag.* **1997**, *45*, 1348–1356. [[CrossRef](#)]
14. Mongia, R.K.; Ittipiboon, A.; Cuhaci, M.; Roscoe, D. Circularly polarized dielectric resonator antenna. *Electron. Lett.* **1994**, *30*, 1361–1362. [[CrossRef](#)]
15. Leung, K.W.; Wong, W.C.; Luk, K.M.; Yung, E.K.N. Circularly polarised dielectric resonator antenna excited by dual conformal strips. *Electron. Lett.* **2000**, *36*, 484–486. [[CrossRef](#)]
16. Wong, W.C.; Leung, K.W. Circularly polarized dielectric resonator antenna excited by dual conformal strips of unequal lengths. *Microw. Opt. Technol. Lett.* **2001**, *29*, 348–350. [[CrossRef](#)]
17. Altaf, A.; Yang, Y.; Lee, K.-Y.; Hwang, K.C. Circularly polarized spidron fractal dielectric resonator antenna. *IEEE Antennas Wireless Propag. Lett.* **2015**, *14*, 1806–1809. [[CrossRef](#)]
18. Abdulmajid, A.A.; Khalil, Y.; Khamas, S. Higher-order-mode circularly polarized two-layer rectangular dielectric resonator antenna. *IEEE Antennas Wirel. Propag. Lett.* **2018**, *17*, 1114–1117. [[CrossRef](#)]
19. Yang, M.; Pan, Y.; Yang, W. A Singly Fed Wideband Circularly Polarized Dielectric Resonator Antenna. *IEEE Antennas Wirel. Propag. Lett.* **2018**, *17*, 1515–1518. [[CrossRef](#)]
20. Elahi, M.; Altaf, A.; Yang, Y.; Lee, K.-Y.; Hwang, K.C. Circularly Polarized Dielectric Resonator Antenna with Two Annular Vias. *IEEE Access* **2021**, *9*, 41123–41128. [[CrossRef](#)]
21. Gupta, A.; Gangwar, R.K. Dual-Band Circularly Polarized Aperture Coupled Rectangular Dielectric Resonator Antenna for Wireless Applications. *IEEE Access* **2018**, *6*, 11388–11396. [[CrossRef](#)]
22. Wang, X.; Sun, L.; Lu, X.; Liang, S.; Lu, W. Single-Feed Dual-Band Circularly Polarized Dielectric Resonator Antenna for CNSS Applications. *IEEE Trans. Antennas Propag.* **2017**, *65*, 4283–4287. [[CrossRef](#)]
23. Weiland, T. Time domain electromagnetic field computation with finite difference methods. *Int. J. Numer. Model. Electron. Netw. Devices* **1996**, *9*, 295–319. [[CrossRef](#)]
24. Yang, M.; Pan, Y.; Sun, Y.; Leung, K. Wideband Circularly Polarized Substrate-Integrated Embedded Dielectric Resonator Antenna for Millimeter-Wave Applications. *IEEE Trans. Antennas Propag.* **2020**, *68*, 1145–1150. [[CrossRef](#)]
25. Trinh-Van, S.; Yang, Y.; Lee, K.; Hwang, K.C. Single-Fed Circularly Polarized Dielectric Resonator Antenna With an Enhanced Axial Ratio Bandwidth and Enhanced Gain. *IEEE Access* **2020**, *8*, 41045–41052. [[CrossRef](#)]
26. Sulaiman, M.I.; Khamas, S.K. A Singly Fed Rectangular Dielectric Resonator Antenna with a Wideband Circular Polarization. *IEEE Antennas Wirel. Propag. Lett.* **2010**, *9*, 615–618. [[CrossRef](#)]
27. Li, B.; Leung, K.W. Strip-fed rectangular dielectric resonator antennas with/without a parasitic patch. *IEEE Trans. Antennas Propag.* **2005**, *53*, 2200–2207.
28. Petosa, A.; Thirakoune, S. Rectangular Dielectric Resonator Antennas with Enhanced Gain. *IEEE Trans. Antennas Propag.* **2011**, *59*, 1385–1389. [[CrossRef](#)]